ECASIA special issue paper

SURFACE and INTERFACE ANALYSIS

Received: 31 August 2013 Revised: 10 December 2013 Accepted: 13 December 2013 Published online in Wiley Online Library: 5 February 2014

(wileyonlinelibrary.com) DOI 10.1002/sia.5381

Characterization of IgG-protein-coated polymeric nanoparticles using complementary particle sizing techniques†

C. Minelli,[a]* R. Garcia-Diez,[b] A. E. Sikora,[a] C. Gollwitzer,[b] M. Krumrey[b] and A. G. Shard[a]

When nanoparticles are introduced into biological media, they acquire a protein corona. The thickness of immunoglobulin G protein on 105 nm polystyrene particles has been determined by dynamic light scattering (DLS), differential centrifugal sedimentation (DCS) and small-angle X-ray scattering (SAXS). All three techniques measured an increase of the protein shell thickness with increasing concentration of the proteins during incubation with the nanoparticles. DLS measurements showed the highest increase, indicating a possible effect of particle agglomeration on the DLS results. DCS accuracy critically depends on the knowledge of the protein shell density but the data allows an estimation of the effective shell density when the thickness was independently determined. SAXS measurements revealed the complex core/shell structure of the bare polystyrene particles. © 2014 Crown Copyright. *Surface and Interface Analysis* © 2014 John Wiley & Sons Ltd.

Keywords: nanoparticle; size measurement; protein coating; core/shell; DLS; DCS; SAXS; DTT

Introduction

Nanoparticle-enabled approaches to the development of innovative medical solutions rely on a high level of particle surface engineering. In addition, when particles are introduced into a biological environment, a dynamic process of protein adsorption and desorption occurs at their surface, which leads to the formation of the so called protein corona surrounding the nanoparticles.[1–5] The identity of the protein corona is found to depend on the nanoparticle size, surface chemistry and surface charge.[2,5,6] The interface of the nanoparticles with their surrounding is therefore complex and its detailed description challenging. Yet, the ability to quantitatively characterise this interface is important in understanding particle behaviour in these complex environments and improving their surface engineering for enhanced functionality.

The use of a combination of particle characterization techniques based upon different physical principles is useful in providing detailed particle characterization. For example, the combination of differential centrifugal sedimentation (DCS) with light-scattering-based particle sizing techniques allows the measurement of size and density of nanoparticles.[7,8] For core/shell systems, where the shell is, e.g. constituted by proteins, such an approach can provide the amount of protein adsorbed on the surface of nanoparticles.[8] In the case of silver and gold nanoparticles, this quantitation can be facilitated through the measurement of their localised surface plasmon resonance, whose wavelength shifts depend on the thickness and the density (i.e. the refractive index) of the protein coating.[4,8,9]

When the particles are of a material other than silver or gold, quantification is more challenging. In this work, we characterise commercially available polystyrene nanoparticles coated with immunoglobulin G (IgG) by combining the use of particle sizing techniques such as dynamic light scattering (DLS), DCS and small-angle X-ray scattering (SAXS). Polystyrene nanoparticles are commonly used in the development of nanoparticle-based strategies for medicine, thanks to the low cost of their material, the versatility of their surface functionalization, the possibility to load them with fluorescent dyes and their availability in narrow size distributions.[10–16] In many of their applications, e.g. biosensing, polystyrene nanoparticles are conjugated with biomolecules and used in biological media.[10,16] The design and control of their function in these complex media requires an in depth understanding of their interface with the environment, e.g. in terms of quantitative description of the biomolecules at their surface. However, because of the polymeric core, the amount of protein at the surface cannot be measured by localised surface plasmon resonance. The task is complicated by the fact that commercially available polystyrene particles may comprise two or more materials and their surface properties depend on their functionalisation. Modelling of such particles is therefore not straightforward as their detailed chemical structure is unknown. While DLS provides accurate results of the hydrodynamic size of these spherical particles, comprising their polymeric core and the surrounding protein shell, DCS relies on knowledge

* *Correspondence to: C. Minelli, Analytical Science, National Physical Laboratory, Hampton road, TW11 0LW Teddington, UK.*
E-mail: caterina.minelli@npl.co.uk

† *Paper published as part of the ECASIA 2013 special issue.*

a *Analytical Science, National Physical Laboratory, Hampton road, TW11 0LW Teddington, UK*

b *Physikalisch-Technische Bundesanstalt (PTB), Abbestr. 2-12, 10587 Berlin, Germany*

of the density of the particle core and that of the protein shell. SAXS enables traceable particle size measurements for sufficiently monodisperse particles and is a powerful tool to determine their size distribution in terms of size and polydispersity,[17] although it relies upon correct modelling for core/shell particles. We compare the particle diameters and protein shell thicknesses obtained with all three methods and discuss their limitations.

Materials and methods

Polystyrene nanoparticles with carboxylated surfaces and a nominal diameter of 105 nm were purchased from Kisker Biotech (Steinfurt, Germany). A set of four IgG-coated polystyrene nanoparticle samples was prepared by incubating 0.05 % (w/w) particles with varying concentrations of IgG from 0.5 to 4 g L^{-1} in 100 mM Tris buffer at pH 8 under continuous shaking for 2 h. Any unbound IgG was then removed from the particle samples by three cycles of centrifugation and redispersion in clean buffer. The use of 6 mM dithiothreitol (DTT) in IgG-coated particle samples was investigated. A sample of aggregated IgG-coated particles ($\rho_{IgG} = 0.5$ g L^{-1}) was incubated in a 6 mM DTT solution for 15 min. An additional set of IgG-coated particles ($\rho_{IgG} = 2$ g L^{-1}) was produced to study the effect of DTT by incubating them in a 6 mM DTT solution for 20 min and 24 h respectively.

DLS and ζ-potential measurements were conducted on a Zetasizer Nano-ZS 3600 instrument (Malvern Instruments Ltd., Malvern, UK) using disposable capillary cells. Measurements were performed in triplicate. The thickness of the protein shell, T_{DLS}, was calculated as half the difference between the diameter measured for the IgG-coated particles and that of the bare polystyrene particles.

DCS measurements were performed with a CPS 20000 instrument (CPS Instruments Inc., Prairieville (LA)), using sucrose gradient with average density $\rho_f = 1.013$ g cm^{-3}, disc angular frequency 2×10^4 rpm, injection volume of 100 µl and 223 nm poly(vinyl chloride) calibration particles of density 1.385 g cm^{-3} provided by the manufacturer. The extinction-intensity-based mode of the particle size distribution was utilised as a measurement of the particle Stokes' diameter. DCS measures particle size on the basis of their sedimentation rate, which depends upon their size and density. Acquisition of a protein layer on a particle changes both the particle volume and density. The thickness of the protein shell is measured by solving the Stokes' equation for a core/shell system,[8] when the particle core diameter and density and the shell density are known. Measurements were performed in triplicate.

SAXS measurements were performed with synchrotron radiation at the four-crystal monochromator beamline in the PTB laboratory at the electron storage ring BESSY II[18] (Berlin, Germany) with a photon energy of $E = (8000.0 \pm 0.5)$ eV. 5 mM DTT were added to the IgG-coated nanoparticles to avoid radiation damage, and after 15 min, the samples were filled into vacuum-proof glass capillaries and inserted into a high vacuum chamber. A vacuum-compatible Pilatus 1 M hybrid pixel detector (Dectris Ltd, Baden, Switzerland) with a pixel size of $d = (172.1 \pm 0.2)$ µm collected the scattered X-ray photons at a distance $L = (4551 \pm 1)$ mm from the capillaries. The recorded scattering patterns consist of concentric rings of different intensities with radii r, which were circularly integrated and converted to momentum transfer q using

$$q = \frac{4\pi E}{hc} \sin\left[\frac{1}{2}\arctan\left(\frac{r}{L}\right)\right] \quad (1)$$

where h is the Planck constant and c is the speed of light. The obtained scattering curve was normalised to the incident intensity, and the exposure time and background were corrected by subtracting the normalised scattering curve of the empty capillary, multiplied by the sample transmittance. The incident photon flux and the sample transmittance were measured by means of calibrated semiconductor photodiodes. Analysis of the curves was performed in the Fourier region by fitting the calculated scattered intensity as the sum of background and particle contributions to the data. The scattering curve of the polystyrene particles was modelled as a spherical core–shell system, and for the coated nanoparticles, a spherical double-shell model was utilised, with a compact spherical core and two surrounding spherical shells. For both cases, a Gaussian size distribution was assumed and the core radius, shell thickness and electron density contrast were treated as fitting parameters.

X-ray photoelectron spectroscopy spectra were taken by an Axis-Ultra XPS instrument (Kratos Analytical, Manchester, UK) using a monochromatic Al Kα *X*-rays at a photon energy of 1486 eV. Samples were prepared by spin coating a 5 % (w/w) particle solution on a gold substrate, and wide and narrow scan regions were acquired from three separate areas at take-off angle normal to the analyser.

Results and discussion

Analysis of the bare polystyrene particles

Table 1 summarises the size measurements performed on the bare polystyrene nanoparticles by DLS, SAXS and DCS. While the SAXS and DLS results are close to the nominal size provided by the manufacturer (i.e. 105 nm), the DCS result is significantly higher. Unlike DLS and SAXS, DCS critically depends on the knowledge of the particle density, which was assumed to be that of polystyrene, i.e. 1.052 g cm^{-3}. DCS can also be used to measure the effective average density of the particles, if their size is known. Assuming the nominal size of 105 nm, we find a particle density of about 1.068 g cm^{-3}, which is 1.5 % higher than that the nominal density of polystyrene. The SAXS data were found to be described best by a core–shell structure of the particles, consisting of a polystyrene core and a shell of higher density.[19] The particles are in fact manufactured following a multiple-addition emulsion polymerisation process using a styrene, methacrylic acid (MAA) and methylmethacrylate (MMA) monomer mix.[20] The MAA or MMA monomers of the resulting copolymer structure are likely to enrich the particle surface because of their decreased hydrophobicity compared with polystyrene, imparting the structure of a core/shell type particle, even though the synthetic polymerisation process is not that of conventional core/shell particles. The particle structure affects the following analysis of the protein-coated particles by DCS and SAXS, which

Table 1. Size measurements of the polystyrene core particles by dynamic light scattering (DLS), differential centrifugal sedimentation (DCS) and small-angle X-ray scattering (SAXS)

Technique	Particle diameter (nm)	Remarks
DLS	102 ± 3	Hydrodynamic diameter
SAXS	110 ± 3	Assuming a core/shell model
DCS	124 ± 2	Assuming 1.052 g cm^{-3} particle density

are model-dependent techniques. While DCS analysis can be carried out by simply assuming an effective core density of 1.068 g cm^{-3}, the SAXS data were modelled with a constant density for core and shell and a stepwise density change in between, although a multi-addition emulsion polymerization synthesis process suggests a more complex interlayer density structure.[19,21,22]

Accurate knowledge of the surface chemical composition of nanoparticles is fundamental for the understanding of nanoparticle interaction with the environment, e.g. in studies aiming at elucidating the correlation between nanoparticles' properties and protein corona formation.[2] ζ-potential measurements alone lack chemical specificity, while surface analysis techniques such as XPS or time-of-flight secondary ion mass spectroscopy are recommended for nanoparticles' surface chemical investigation.[23]

The presence of MMA and MAA monomers at the surface of the particles was thus confirmed by the XPS study. Figure 1 shows the XPS C 1 s spectrum of the particle sample, where the contributions of the MMA and MAA are highlighted with dashed lines. XPS detects electrons escaped from the top ~10 nm of the material's surface and thus describes the chemistry of the outer shell of the particles. Polystyrene contributes to the main hydrocarbon peak at 285 eV and the shake-up peaks at about 292 eV due to $\pi \rightarrow \pi^*$ transitions of the aromatic ring.[24] The presence of the peak at 289.5 eV distinctive of the carboxyl group (COO) clearly indicates the presence of MAA or MMA monomers, the best fit to the C 1 s spectrum indicating the presence of a mixture of the two co-monomers.

Analysis of the IgG-coated polymer particles

Table 2 summarises results obtained for the IgG-coated particle systems, where the uncertainties are the standard deviations of repeated measurements. Because of the surface carboxylation, the bare polystyrene particles are highly negatively charged, with ζ-potential of (−49 ± 1) mV. Following the formation of the protein coating, the ζ-potential of the particles increases to around −10 mV.

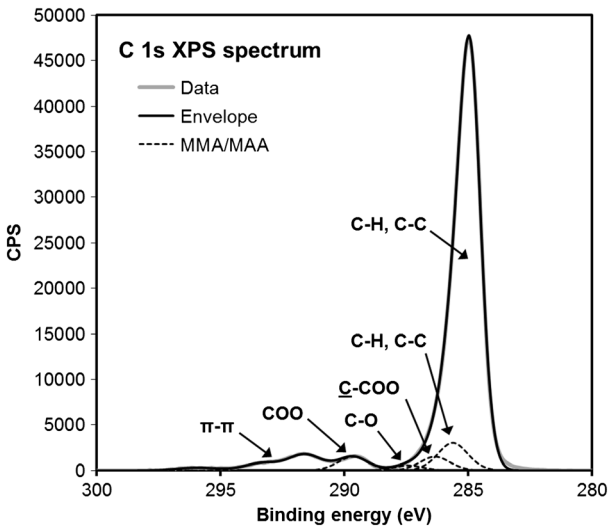

Figure 1. X-ray photoelectron spectroscopy (XPS) C 1 s spectrum of the bare polymer particles. The particles are mainly composed of polystyrene, which contributes to the main hydrocarbon peak at 285 eV and the shake-up $\pi \rightarrow \pi^*$ peaks at about 292 eV. The peaks attributed to methylmethacrylate (MMA) and methacrylic acid (MAA) co-monomers are highlighted with dashed lines.

Table 2. Measurement of the immunoglobulin G (IgG) shell thickness by dynamic light scattering (DLS), differential centrifugal sedimentation (DCS) and small-angle X-ray scattering (SAXS)

Sample	ρ_{IgG} (g L^{-1})	ζ-potential* (mV)	T_{DLS} (nm)	T_{DCS} ** (nm)	T_{SAXS} (nm)
PS1	0.5	−10.8 ± 0.9	10 ± 1	3.7 ± 0.6	7.7 ± 1.4
PS2	1	−10.7 ± 0.6	11 ± 2	5.9 ± 0.5	8.4 ± 1.4
PS3	2	−9.6 ± 0.5	12 ± 2	7.6 ± 0.4	9.6 ± 1.5
PS4	4	−9.7 ± 0.5	15 ± 2	8.3 ± 0.4	9.6 ± 1.5

* ζ-potential of bare polystyrene particles is (−49 ± 1) mV.
** Assuming $\rho_{eff} = 1.068$ g cm^{-3} and $\rho_s = 1.125$ g cm^{-3}.

All three techniques show an increase in the IgG shell thickness with increasing concentration of the protein in solution during incubation, where thicknesses ranged from 10 to 15 nm and 7.7 to 9.6 nm for DLS and SAXS respectively. The shell thickness measured by DCS depends on the value chosen for shell density. When the value 1.125 g cm^{-3} in accordance with a previous estimate[3] is used, the measured thickness ranged between 3.7 and 8.3 nm. These results suggest that a monolayer of antibodies is formed around the particles and possibly additional IgG molecules adsorb on such a layer when higher protein concentrations were used.[25] DLS provided higher values than the other techniques, indicating that the measurement of the diameter of the IgG-coated particles may have been overestimated because of the presence of agglomerated particles in the sample. Analysis of the width of the particle size distributions as measured by DLS and DCS supports this hypothesis: although an increase in the polydispersity index from 0.016 ± 0.010 for the bare particle to a maximum of 0.051 ± 0.004 for PS1 was found by DLS, DCS results did not show any significant change in the width of the size distributions of the primary particle populations for the coated and uncoated samples. However, the presence of small aggregates was observed in the coated samples, as shown in Fig. 2.

Comparison of the shell thickness values measured by DCS and SAXS seems to indicate an effective protein shell density slightly lower than 1.125 g cm^{-3}. SAXS results were obtained using a double-shell approach to model the IgG-coated nanoparticles, focusing on the total diameter instead of the details of the internal structure. Here, the limits of the inner and outer radii of the polymer shell are not fixed to account for a possible diffuse density profile and are treated as fitting parameters together with the outer radius and the contrast difference of each shell with the polystyrene core. Although all techniques show an increase of the IgG shell thickness with increasing concentration of the protein, full consistency among them requires further refinements of the SAXS and DCS modelling.

Effect of DTT on IgG-coated polystyrene particles

Dithiothreitol is utilised in samples undergoing SAXS analysis as a free radical scavenger, preventing the sample from X-ray radiation damage.[26] When the incident photons react with the solvent, they create hydroxyl radicals that attack proteins inducing radiation-induced aggregates. Accurate size measurements by DLS and SAXS also require the samples to be free from aggregates, and DTT has the ability to break disulphide bonds formed between IgG molecules belonging to the shell of different particles. However, depending on its concentration and incubation time, DTT can also potentially affect the protein shell formed

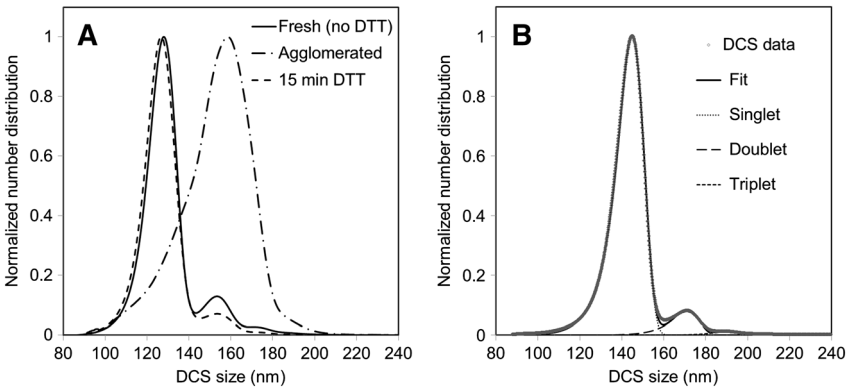

Figure 2. (A) Normalised number size distributions measured by differential centrifugal sedimentation (DCS) technique of immunoglobulin G (IgG)-coated polymer nanoparticles ($\rho_{IgG} = 0.5\ g\ L^{-1}$) freshly prepared (continuous line), agglomerated (dash-dot line) and after 15 min incubation in 6 mM dithiothreitol (DTT) (dash line). (B) Example of fitting of the normalised number size distributions measured by DCS technique of freshly prepared IgG-coated polymer nanoparticles ($\rho_{IgG} = 2\ g\ L^{-1}$). The particles were modelled as uniform spheres of density $1.068\ g\ cm^{-3}$.

around the nanoparticles. For these reasons, the effect of 6 mM DTT on the IgG-coated particle sample was investigated. DTT in concentrations between 1 and 10 mM is in fact typically used as a protein-reducing agent[27] and as a free radical scavenger in SAXS experiments.[28] The investigation was performed using DCS, because of the high resolution of particle size distributions. We first studied the effect of DTT on an aggregated sample. Figure 2(A) shows the DCS number distributions of a fresh sample with no DTT, the same sample when agglomerated and after subsequent incubation in 6 mM DTT for 15 min. The fresh sample distribution exhibits a main mode around 156 nm and a second peak at 186 nm (doublets) followed by a tail at higher particle size values. The secondary peak can be confidently assigned to the clustered particles because their position relative to the main single-particle mode can be calculated. The DCS size distribution was thus modelled as the sum of distributions of clustered and non-clustered particles [see Fig. 2(B) for example]. The fit of the model indicates that for the fresh sample, about 27 % of the particles are agglomerated in clusters of two (~19 %) or more. The aggregated sample has a broader size distribution, with the main mode at the position of the particle doublets and a significant tail related to larger clusters. After 15 min incubation in DTT, the same sample undergoes a dramatic change in size distribution, which is now restored to that of the fresh sample. DTT is thus effective in breaking the bonds between the nanoparticles, which supports the hypothesis that these are mainly due to disulphide bonds established between antibodies from the shells of different nanoparticles. It is interesting to observe that in this last sample, the clustered particles comprise 16 % of the total sample, which is less than that observed in the fresh sample. This result suggests that the use of DTT may be beneficial also in fresh samples as it decreases the amount of cluster particles. The effect of DTT was therefore also investigated on freshly prepared samples. Here, the percentage of clustered nanoparticles was reduced from 18 % to 8 % with 20 min of incubation and reached 6 % after 24 h. No significant shift was observed in the position of the main mode of the particle size distribution, indicating that 6 mM DTT did not affect significantly the IgG coating surrounding the particles in the investigated time range. This result indicates that DTT is effective in improving samples' monodispersity without affecting their structure, which is highly desirable in techniques such as SAXS, where narrow size distributions are required to observe the characteristic minima at the Fourier region, or DLS, where the intensity-weighted size distributions would provide an overestimate of the average particle size because of the strong dependence between particle size and light scattering.

Conclusions

The use of complementary techniques such as DLS, SAXS and DCS is a powerful approach to detail the complex structure of protein-coated nanoparticles. The core/shell nature of the polymer particle was revealed and characterised. All techniques show an increase of the IgG shell thickness with increasing concentration of the proteins during incubation with the nanoparticles, but model refinement is required for their full consistency. We also showed that DTT is effective in reducing agglomeration among nanoparticles without affecting the protein corona and its use is compatible with SAXS, where it is used as a radical scavenger.

Acknowledgements

This work forms part of the Chemical and Biological and Innovation Research and Development programmes of the National Measurement System of the UK Department of Business, Innovation and Skills, with additional funding by the European Union through the European Metrology Research Programme (EMRP). The EMRP is jointly funded by the EMRP participating countries within EURAMET and the European Union.

References

[1] T. Cedervall, I. Lynch, S. Lindman, T. Berggard, E. Thulin, H. Nilsson, K. A. Dawson, S. Linse, *Proc. Natl. Acad. Sci. U. S. A.* **2007**, *104*, 2050.
[2] M. Lundqvist, J. Stigler, G. Elia, I. Lynch, T. Cedervall, K. A. Dawson, *Proc. Natl. Acad. Sci. U. S. A.* **2008**, *105*, 14265.
[3] M. P. Monopoli, D. Walczyk, A. Campbell, G. Elia, I. Lynch, F. Baldelli Bombelli, K. A. Dawson, *J. Am. Chem. Soc.* **2011**, *133*, 2525.
[4] E. Casals, T. Pfaller, A. Duschl, G. J. Oostingh, V. Puntes, *ACS Nano* **2010**, *4*, 3623.
[5] S. Tenzer, D. Docter, J. Kuharev, A. Musyanovych, V. Fetz, R. Hecht, F. Schlenk, D. Fischer, K. Kiouptsi, C. Reinhardt, K. Landfester, H. Schild, M. Maskos, S. K. Knauer, R. H. Stauber, *Nat. Nanotechnol.* **2013**, *8*, 772.
[6] A. Gessner, A. Lieske, B.-R. Paulke, R. H. Müller, *J. Biomed. Mater. Res. A* **2003**, *65A*, 319.
[7] N. C. Bell, C. Minelli, J. Tompkins, M. M. Stevens, A. G. Shard, *Langmuir* **2012**, *28*, 10860.
[8] N. C. Bell, C. Minelli, A. G. Shard, *Anal. Methods* **2013**, *5*, 4591.
[9] K. Kaur, J. A. Forrest, *Langmuir* **2012**, *28*, 2736.

[10] K. Nielsen, W. L. Yu, M. Lin, S. A. N. Davis, C. Elmgren, R. MacKenzie, J. Tanha, S. Li, G. Dubuc, E. G. Brown, L. Keleta, J. Pasick, *J. Immunoassay Immunochem.* **2007**, *28*, 307.
[11] E. M. Linares, L. T. Kubota, J. Michaelis, S. Thalhammer, *J. Immunol. Methods* **2012**, *375*, 264.
[12] I. Nakhla, H. El Mohammady, A. Mansour, J. D. Klena, K. Hassan, Y. Sultan, R. Pastoor, T. H. Abdoel, H. Smits, *Diagn. Microbiol. Infect. Dis.* **2011**, *70*, 435.
[13] K. Svoboda, S. M. Block, *Annu. Rev. Biophys. Biomol. Struct.* **1994**, *23*, 247.
[14] G. J. Randolph, K. Inaba, D. F. Robbiani, R. M. Steinman, W. A. Muller, *Immunity* **1999**, *11*, 753.
[15] H. Morgan, M. P. Hughes, N. G. Green, *Biophys. J.* **1999**, *77*, 516.
[16] G. J. Worsley, S. L. Attree, J. E. Noble, A. M. Horgan, *Biosens. Bioelectron.* **2012**, *34*, 215.
[17] F. Meli, T. Klein, E. Buhr, C. G. Frase, G. Gleber, M. Krumrey, A. Duta, S. Duta, V. Korpelainen, R. Bellotti, G. B. Picotto, R. D. Boyd, A. Cuenat, *Meas. Sci. Technol.* **2012**, *23*, 125005.
[18] M. Krumrey, G. Gleber, F. Scholze, J. Wernecke, *Meas. Sci. Technol.* **2011**, *22*, 094032.
[19] R. Grunder, G. Urban, M. Ballauff, *Colloid Polym. Sci.* **1993**, *271*, 563.
[20] Kisker Biotech (Steinfurt - Germany), **2013**.
[21] W. D. Hergeth, U. J. Steinau, H. J. Bittrich, H. Tanneberger, *Colloid Polym. Sci.* **1990**, *268*, 991.
[22] D. Beyer, W. Lebek, W. D. Hergeth, K. Schmutzler, *Colloid Polym. Sci.* **1990**, *268*, 744.
[23] D. R. Baer, M. H. Engelhard, G. E. Johnson, J. Laskin, J. Lai, K. Mueller, P. Munusamy, S. Thevuthasan, H. Wang, N. Washton, A. Elder, B. L. Baisch, A. Karakoti, S. V. N. T. Kuchibhatla, D. Moon, *J. Vac. Sci. Technol. A* **2013**, *31*, 050820.
[24] C. Girardeaux, J.-J. Pireaux, *Surf. Sci. Spectra* **1996**, *4*, 130.
[25] Y. H. Tan, M. Liu, B. Nolting, J. G. Go, J. Gervay-Hague, G.-Y. Liu, *ACS Nano* **2008**, *2*, 2374.
[26] S. Kuwamoto, S. Akiyama, T. Fujisawa, *J. Synchrotron Radiat.* **2004**, *11*, 462.
[27] W. W. Cleland, *Biochemistry* **1964**, *3*, 480.
[28] G. L. Hura, A. L. Menon, M. Hammel, R. P. Rambo, F. L. Poole, S. E. Tsutakawa, F. E. Jenney, S. Classen, K. A. Frankel, R. C. Hopkins, S. J. Yang, J. W. Scott, B. D. Dillard, M. W. W. Adams, J. A. Tainer, *Nat. Methods* **2009**, *6*, 606.